Helmut Hörner, Samuel Rind, Sita Schönbauer

Praktikum Quantenphysik 141.A12
Pulsed Nuclear Magnetic Resonance

Lab Report

(Rev. 2)

Vienna University of Technology
Institute of Atomic and Subatomic Physics

Vienna, May 2019

Contents

1 Introduction

The experiments described in this report were carried out by Samuel Rind, Sita Schönbauer and Helmut Hörner on May 9, 2019 at the Institute of Atomic and Subatomic Physics of the Vienna University of Technology as part of the course "Praktikum Quantenphysik 141.A12". The experiments demonstrate the principles of nuclear magnetic resonance (NMR).

2 Experiments

2.1 Lamor Frequency of Protons in the Hydrogen Atoms of Mineral Oil

2.1.1 Theory and Experimental Setup

In this series of experiments, mineral oil was exposed to a static, homogeneous magnetic field $\vec{B_0} = B_0\vec{e}_z$ of a NdFeB permanent magnet. As the liquid consists of hydrocarbons, in which the ^{12}C nuclei have no spin, this leads to a precession of the spins of the protons in the hydrogen atoms around the z-axis with the angular Lamor frequency

$$\omega_L = \gamma B_0 \tag{1}$$

When exposed to such a magnetic field, spins aligned along the applied magnetic field $\vec{B_0}$ have a lower energy than spins pointing in the opposite direction, with the energy difference being $\Delta E = \hbar\omega$ ("Nuclear Zeeman Effect"). The difference in population between these two states is only on the ppm order, but yet strong enough to be observed as a net magnetization $\vec{M_0}$.

In this experimental setup, in addition to the static $\vec{B_0}$ field, also a pair of Helmholtz-coils (integrated in [PS2 RF Sample Probe]) was placed around the sample so that it could be exposed to RF pulses $\vec{B}_{RF} = B_1 \cos(\omega t)\vec{e}_x$ perpendicular to the $\vec{B_0}$ field (hereby defining the as x-axis).

When $\omega = \omega_L$, then there is resonance, and the effect of the (comparably small) $\vec{B}_{RF}$ field can accumulate with every full precession cycle and can hence give rise to a large change in the spin state, and consequently in the net magnetization vector (see [Levitt 2008, p.247]). For example, if the RF pulse is timed so that $t_{RF}\omega_L = \frac{\pi}{2}$, then the net magnetization vector will be processing around the equator at the Lamor frequency ("$\frac{\pi}{2}$-pulse"). Similarly, a π-pulse will move the net magnetization vector further towards the negative z-direction, and so on.

The precessing spins induce an electric current in the Helmholtz-coils (which also dub as detectors). This signal is maximal when the rotation axis of the net magnetic momentum lies perpendicular to the magnetic axis of the coils, i.e. when the net magnetization vector is processing around the equator.

The Helmholtz Coils in [PS2 RF Sample Probe] were connected to a [PS2 Mainframe] programmable pulse sequence RF pulse generator.

The current induced by the protons RF-field was processed into two separate signals, which where displayed in parallel by a [DSO-X 2012A] oscilloscope: On channel 1, the *envelope of the signal emitted by the protons* was displayed, and on channel 2 the *real part of the interference signal* between the RF-pulse emitted into the sample and the RF-pulse received from the sample was displayed.

The pulse generator [PS2 Mainframe] was set to generate 1 µs pulses with a 300 ms period (to allow complete thermalization between the pulses). The oscilloscope trigger input was connected to the pulse generator.

2.1.2 Experimental Results

On channel 2 of the [DSO-X 2012A] oscilloscope (showing the phase difference between emitted and received signal), a damped oscillation, representing the beat between the precessing magnetization vector and the RD frequency applied in the pulse, became visible. The frequency of the RF pulse generator was tuned until the beat oscillation vanished.

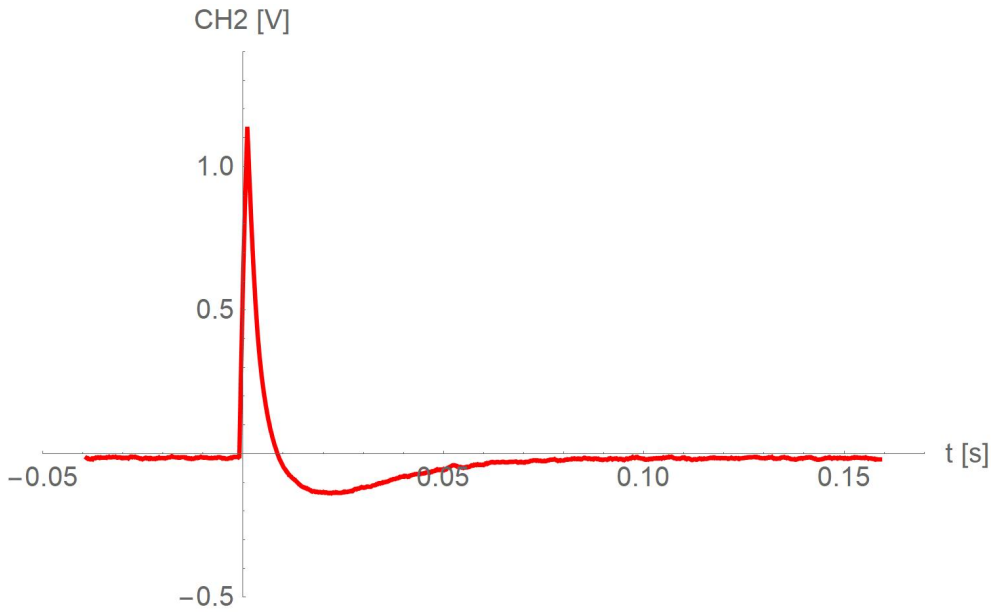

Figure 1: Beat oscillation vanished after RF pulses tuned to Lamor frequency

The resonance frequency was measured to be

$$f_{res} = f_L = 21.524\,19\,\mathrm{MHz} \tag{2}$$

Considering that $\omega_L = 2\pi f_L$, equation (1) can be rearranged to

$$B_0 = \frac{2\pi f_L}{\gamma} \tag{3}$$

With the gyromagnetic ratio of the proton being $\gamma = 267.522 \times 10^6\,\frac{\mathrm{rad}}{\mathrm{s\,T}}$, the value of the magnetic field $\vec{B_0}$ can be calculated to be

$$B_0 = 0.506\,\mathrm{T} \tag{4}$$

2.2 Fine-Tuning the Magnetic Field

2.2.1 Theory and Experimental Setup

To make the magnetic field $\vec{B_0}$ as homogeneous over the volume of the sample as possible, gradient coils were placed alongside the permanent magnet. These gradient coils were connected to the [PS2 Controller], which allows for tuning the linear magnetic field gradients along all three axes, as well as for the quadratic filed component along the z-axis. The field is most homogeneous when the envelope signal on channel 1 has the maximum length.

2.2.2 Experimental Results

It turned out that the setting of the [PS2 Controller] was already almost optimal. Therefore, there is only a minuscule difference in the determined value for the Lamor frequency after this tuning step.

$$f_{res} = f_L = 21.524\,47\,\mathrm{MHz} \tag{5}$$

2.3 Manipulating Spin Orientation by Applying Pulses of According Length

2.3.1 Theory and Experimental Setup

In this experiment, we varied the pulse length between 0 µs and 20 µs with a 300 ms period (to allow complete thermalization between the pulses). For each pulse length the immediate peak amplitude of the signals in channel 1 and channel 2 was recorded.

With increasing pulse length, the net magnetization vector moves towards the equator and hence the envelope signal in channel 1 increases from zero to maximum until the $\frac{\pi}{2}$ pulse length is reached. Then the signal strength is expected to decrease to a minimum until the pulse length reaches π pulse length. This cycle then continues with $\frac{3\pi}{2}$ and 2π pulse length. Hence, tuning the pulse length from 0 to 2π results in two signal periods.

In contrast, the phase signal in channel 2 is expected to show only one full period when tuning the pulse length from 0 to 2π pulses.

2.3.2 Experimental Results

Table 1 shows the measured values. As can be seen, two extra measurements were performed "outside" the constant grid to determine the exact pulse lengths for the channel 2 phase signal to become zero. This allows for the most precise calculation of the $\frac{\pi}{2}$ signal length.

Pulse Length μs	CH 1 Envelope V	CH2 Phase Diff. V
0.0	0.000	0.000
1.0	4.188	0.631
2.0	7.250	1.100
4.0	9.870	1.488
6.0	7.750	1.110
8.0	1.000	0.112
8.2	-	0.000
10.0	5.562	-1.000
12.0	8.560	-1.480
14.0	7.630	-1.260
16.0	2.200	-0.410
16.8	-	0.000
18.0	4.080	0.580
20.0	7.250	1.060

Table 1: Signal strength and signal phase difference vs. pulse length

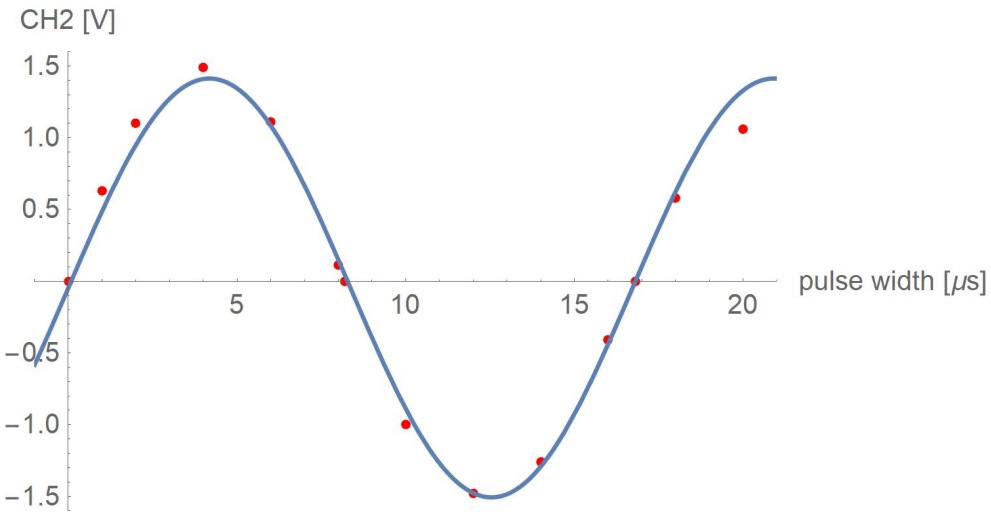

Figure 2: Phase sensitive signal for various pulse widths

As a pulse width of 16.8 µs concludes a full period in the channel 2 phase signal (equaling to a 2π pulse, see table 1), the $\frac{\pi}{2}$ pulse length can easily be calculated to be

$$t_{\pi/4} = \frac{t_\pi}{4} = \frac{16.8}{4} = 4.2\,\mu s \tag{6}$$

2.4 Inhomogeneous Traverse Relaxation Time T_2^*

2.4.1 Theory and Experimental Setup

As the microscopic environment of each nucleus is slightly different, each nucleus has consequently a slightly different Lamor frequency. This means that, after a $\frac{\pi}{2}$ pulse, the spin vectors will spread out more and more over time, until coherence is lost. Furthermore, the applied magnetic field $\vec{B_0}$ is not entirely homogeneous which in total leads to an even increased decoherence speed, characterized by the traverse relaxation time T_2^*

$$M_{trans} = M_0 e^{-t/T_2^*} \tag{7}$$

The traverse relaxation time T_2^* can be determined by exposing the sample to $\frac{\pi}{2}$ pulses, and fitting equation 5 to the measured envelope signal on channel 1.

2.4.2 Experimental Results

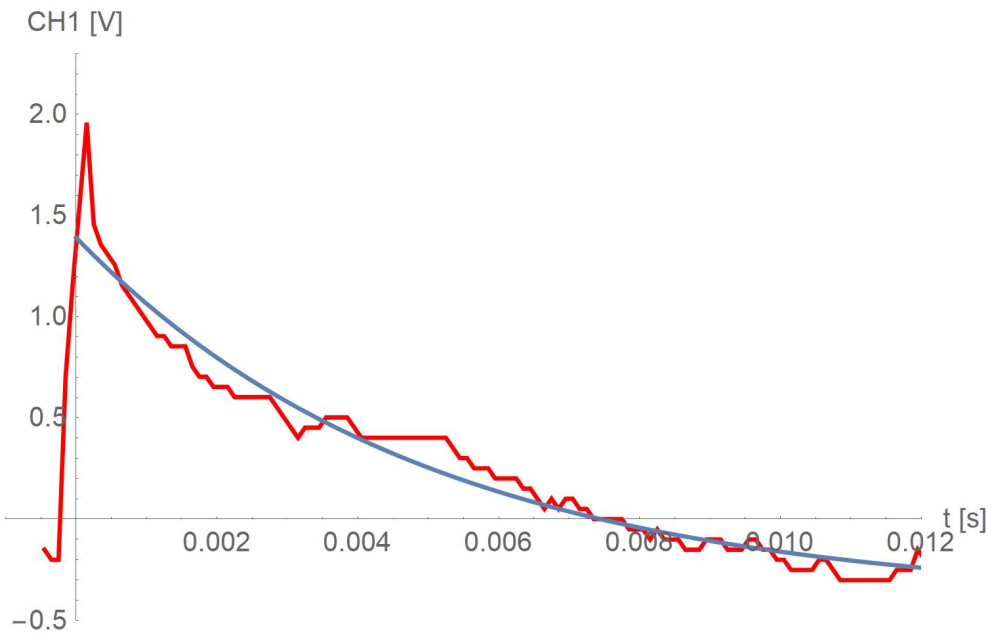

Figure 3: Exponential decay after a $\frac{\pi}{2}$ pulse (red) and fit function $-0.4 + 1.79e^{1/0.005}$

As figure 3 shows, the measured decay in the envelope signal on channel 1 had a certain bias, so that the signal dropped below zero when leveling out. This was accounted for by extending fit-function (7) with a fixed offset of -0.4.

The best-fit function, for which the parameters were determined employing the NonlinearModelFit method of Mathematica 11.3., is $-0.4+1.79e^{1/0.005}$. From this fit function, the estimated traverse relaxation time can be determined to be

$$T_2^* = 5\,\mathrm{ms} \tag{8}$$

2.5 Spin-Lattice Relaxation Time T_1

2.5.1 Theory and Experimental Setup

The previous measurement did not reflect the actual spin-lattice relaxation time T_1, as it was affected by unavoidable inhomogeneities in the magnetic field $\vec{B_0}$. This problem can be circumvented by the "inverse recovery T_1 pulse sequence", employed in the next measurement: In the first step, the sample is exposed to a π pulse, which turns all spins into negative z direction. As time passes, the spins will begin to rotate back towards positive z-direction, ever more spreading out around all φ angles.

Then, after as specific time τ, a further $\frac{\pi}{2}$ pulse is emitted into the sample. This brings the rotating net spin vector to the traverse plane. The projection of the net spin into the xy-plane however will depend on the amount of decoherence the individual spin vectors have experienced in the time τ between the π pulse and the $\frac{\pi}{2}$ pulse. First, the projection of the net spin into the xy-plane will get ever smaller with growing τ. When the $\frac{\pi}{2}$ pulse hits exactly at the moment when the spins have decoherently spread out and moved to the traverse plane anyway ("zero crossing time"), the projection of the net spin into the xy-plane after the $\frac{\pi}{2}$ will be exactly zero.

This means that the phase sensitive signal on channel 2 is expected to start with large negative values for short values of τ and will become ever closer to zero until τ reaches the zero-crossing time. After that, the phase sensitive signal on channel 2 will become positive.

The intensity of the signal is described by

$$M(t) = M_0(1 - 2e^{t/T_1}) \tag{9}$$

The intensity is zero at $\tau_{zero} = T_1 \log(2)$, so that T_1 can easily be determined by measuring the zero-crossing time τ_{zero}

$$T_1 = \frac{\tau_{zero}}{\log(2)} \tag{10}$$

2.5.2 Experimental Results

Table 2 shows the results of the inverse recovery T_1 pulse sequence measurement.

τ ms	CH2 peak V
0,1	-1,46
5,0	-1,09
10,0	-0,66
15,0	-0,34
20,0	-0,16
25,0	0,00
30,0	0,19
35,0	0,39
40,0	0,51
45,0	0,63

Table 2: Inverse recovery T_1 pulse sequence measurement

As can be seen in this table, the zero-crossing time $\tau_{zero} = 25\,\text{ms}$. Employing relation (10), the spin-lattice replaxation time can be calulated to be

$$T_1 = \frac{25\,\text{ms}}{\log(2)} = 36\,\text{ms} \tag{11}$$

The following figure 4 visualizes the complete data set and the matching fit-function $-0.4+1.79e^{1/0.005}$ (parameter determined with the NonlinearModelFit method of Mathematica 11.3).

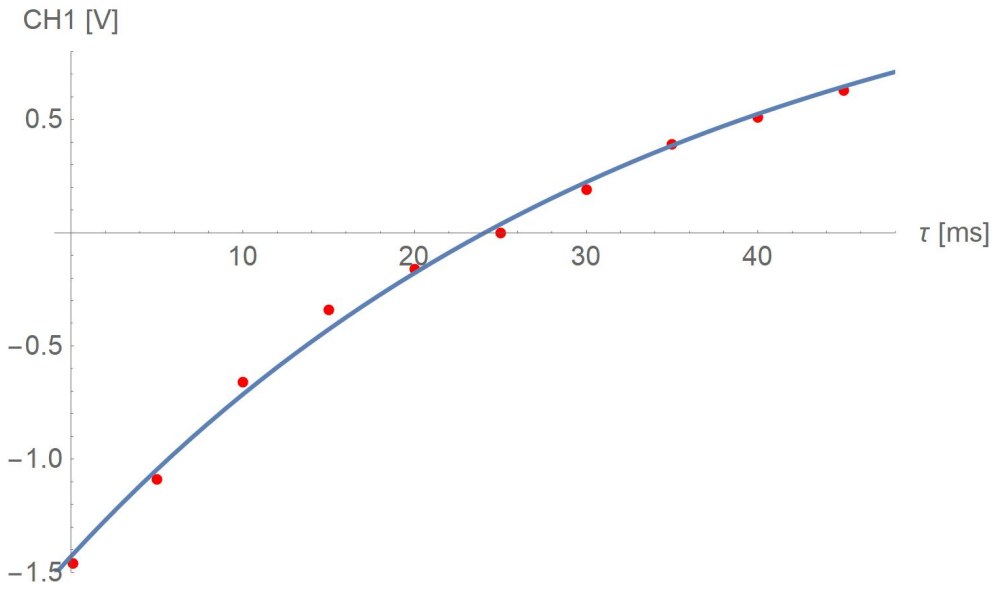

Figure 4: Inverse recovery T_1 pulse sequence measurement; fit-function $1.43(1-2e^{-t/34.7})$

According to the fit-function displayed in above graph, the spin-lattice relaxation time can be estimated to be

$$T_1 = 34.7\,\text{ms} \tag{12}$$

2.6 Homogeneous Traverse Relaxation Time T_2

2.6.1 Theory and Experimental Setup

To determine the exact traverse relaxation time T_2 without having inhomogenities in the magnetic field $\vec{B_0}$ affecting the measurement (as in the measurement of T_2^*), the following method was applied:

With a first $\frac{\pi}{2}$ pulse, the net magnetization was rotated into the equatorial plane. Next, after a certain time τ during the decay, the sample was exposed to another π pulse. This leads to a re-phasing of the spins, visible in so-called "Hahn-Echos" in the envelope signal of channel 1 (see figure 5).

By varying the delay time τ, Hahn-echos of different peak amplitudes can be generated. When the peak values of these Hahn-echos are plotted over τ, and this plot is then fitted by equation 13, the exponent parameter T_2 of the fitting function gives a good estimation of the actual homogeneous traverse relation time.

$$M_{trans} = M_0 e^{-t/T_2} \tag{13}$$

2.6.2 Experimental Results

Figure 5 shows an exemplary Hahn echo after a delay time $\tau = 6\,\text{ms}$

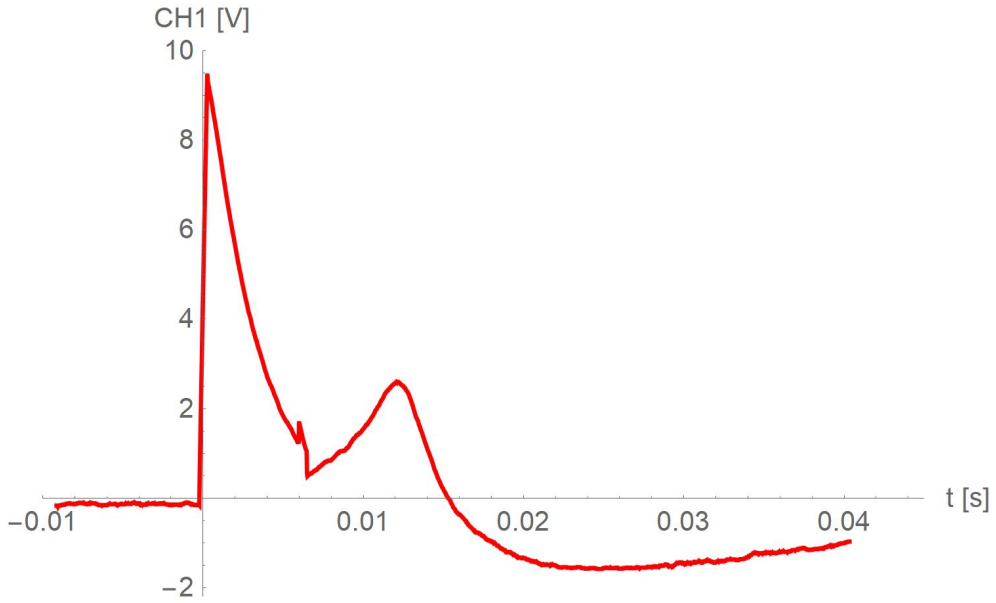

Figure 5: Exemplary Hahn echo after $\tau = 6\,\text{ms}$ in the envelope signal on channel 1

τ ms	CH1 peak V
2,0	5,60
4,0	4,02
6,0	2,80
6,2	2,77
8,0	2,10
10,0	1,57
12,0	1,20
14,0	0,97
16,0	0,80
18,0	0,67
20,0	0,57

Table 3: Magnitude of Hahn echos over different delay times τ

The following figure 6 visualizes the complete data set of table 3 and the matching fit-function $7.4e^{-t/6.7}$ (parameter determined with the NonlinearModelFit method of Mathematica 11.3).

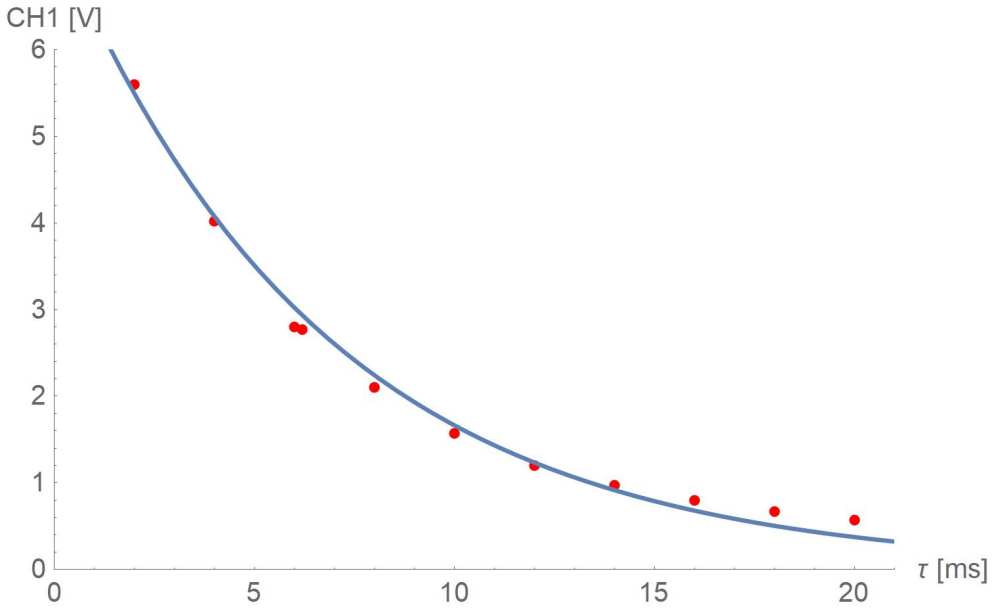

Figure 6: Magnitude of Hahn echo vs. delay time τ; fit-function $7.4e^{-t/6.7}$

From this fit-function, the homogeneous traverse relaxation time T_2 can be determined to be

$$T_2 = 6.7\,\text{ms} \tag{14}$$

which is, as expected, longer than the previously measured inhomogeneous traverse relaxation time $T_2^* = 5\,\text{ms}$.

The relationship between T_2 and "T_2^* is given by

$$\frac{1}{T_2} = \frac{1}{T_2^*} - \frac{\gamma \Delta B_0}{2} \tag{15}$$

with ΔB_0 being the magnetic field inhomogeneity. Equation (15) can be re-arranged to

$$\Delta B_0 = \frac{2}{\gamma}\left(\frac{1}{T_2^*} - \frac{1}{T_2}\right) \tag{16}$$

Hence, the magnetic field inhomogeneity in our experiment was

$$\Delta B_0 = \frac{2}{267.522 \cdot 10^6}\left(\frac{1}{0.005} - \frac{1}{0.0067}\right) = 379\,\text{nT} \tag{17}$$

2.7 Measuring T_2 with Multiple Pulse Sequences

2.7.1 Theory and Experimental Setup

A refinement of the Hahn echo method was described by [Carr and Purcell, 1954]. In this scheme, a first $\frac{\pi}{2}$ pulse is followed by a series of π pulses. If the time interval between the first $\frac{\pi}{2}$ and second π pulse is τ, then the interval between all further impulses has to be 2τ. Echos are observed midway between the π pulses, and the amplitude of successive echos decays exponentially with a time constant equal to T_2.

However, with this method the exact adjustment of the π pulses is crucial, because even small deviations from the exact value gives rise to cumulative errors in the result. This is in conflict with the requirement that the number of π pulses should be large in order to eliminate the effects of diffusion.

An improved pulse sequence named "CPMG" after their developers Carr, Purcell, Meiboom and Gill, described in [Meiboom and Gill, 1958], solves this problem. The pulse sequence differs from the method described by [Carr and Purcell, 1954] in two respects: (i) The successive pulses are coherent, and (ii) the phase of the $\frac{\pi}{2}$ pulse is shifted by $\frac{\pi}{2}$ pulse relative to the pase of the π pulses.

2.7.2 Experimental Results

We programmed the [PS2 Mainframe] to the CPMG sequence with $\tau = 5\,\text{ms}$. Figure 7 visualizes the Hahn echos produced by this sequence and the matching fit-function $-0.28 + 9.97e^{-t/0.0075}$ (parameter determined with the NonlinearModelFit method of Mathematica 11.3).

The time constant extracted from the fit-function gives the T_2 value to be

$$T_2 = 7.5\,\text{ms} \tag{18}$$

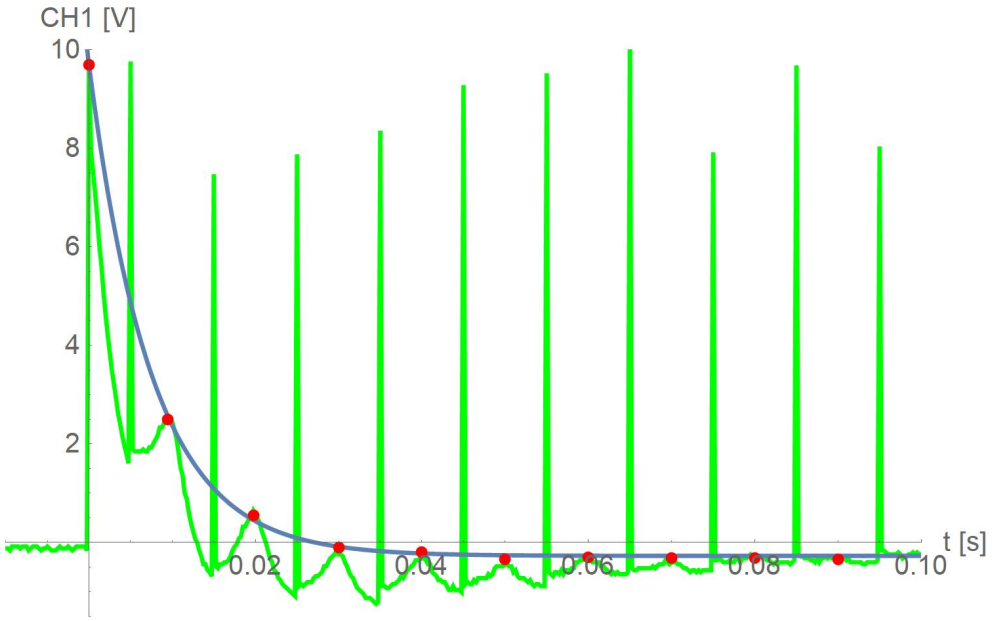

Figure 7: CPMG pulse sequence ($\tau = 5\,\text{ms}$); fit-function $-0.28 + 9.97e^{-t/0.0075}$

3 Appendix

Equipment

[PS2 Controller]	Current regulated supply for gradient coils TeachSpin PS2 Controller
[PS2 Mainframe]	Pulse Programmer/Synthesizer/Receiver unit TeachSpin PS2 Mainframe
[PS2 RF Sample Probe]	Single coil RF sample probe TeachSpin PS2 RF probe
[DSO-X 2012A]	Oscilloscope Keysight InfiniiVision DSO-X 2012A

List of Tables

List of Figures

References

[Carr and Purcell, 1954] Carr, H. Y., Purcell, E. M.; Effects of Diffusion on Free Precession in Nuclear Magnetic Resonance Experiments. Physical Review. 94, 1954, p. 630–638. DOI:10.1103/PhysRev.94.630

[Levitt 2008] Malcom J. Levitt: Spin Dynamics; Basics of Nuclear Magnetic Resonance, 2nd edition, 2008. John Wiley, Chichester.

[Meiboom and Gill, 1958] S. Meiboom and D. Gill; Modified Spin-Echo Method for Measuring Nuclear Relaxation Times, Rev. Sci. Instrum. 29, 688 (1958), DOI: 10.1063/1.1716296